IL NUOVO CIMENTO **38 C** (2015) 62
DOI 10.1393/ncc/i2015-15062-9

COMMUNICATIONS: SIF Congress 2014

Measurement of β^--decay continuum spectrum of ^{138}La

A. GIAZ
INFN, Sezione di Milano - Milano, Italy

received 30 January 2015

Summary. — The $LaBr_3$:Ce scintillator offers the unique opportunity to study the ^{138}La β^- radioactive decay. This decay is a 2nd-order unique forbidden transition. The ^{138}La isotope is one of the rarest isotopes on earth (it is present as 0.09% in natural lanthanum) and it has an extremely long lifetime, of the order of 10^{11} years. Large amounts of ^{138}La are, indeed, needed for the measurement of the β^--decay spectrum. In the literature, only one experimental measurement is present and the results are not reproduced by theoretical calculations. A second measurement of the β^- continuum is presented in this work. For this measurement, two $LaBr_3$:Ce scintillators ($3'' \times 3''$) were used. The measured spectrum β^- is found to be comparable to the one previously measured and published.

PACS 29.40.Mc – Scintillation detectors.
PACS 23.40.-s – β decay; double β decay; electron and muon capture.

1. – Introduction

The aim of this work is the measurement of the energy spectrum of the electron emitted in the β^- decay of the ^{138}La. This is the second measurement ever done so far. The first measurement was performed in Delft by F. Quarati *et al.* and produced two spectra. Two different experimental tecniques were used: the convolution and the decovolution method [1]. The two experimental spectra had small differences and both are not in agreement with the theoretical prediction.

This measurement aims to better investigate the difference between the theoretical spectrum and the experimental data. We propose a new measurement, exploiting the coincidence between the two $3'' \times 3''$ $LaBr_3$:Ce. The $LaBr_3$:Ce detectors contain ^{138}La and they can be used both as a source and as a detector.

In this work, the description of the ^{138}La radioactive decay will be reported in sect. **2**. We will discuss the experimental method used to extract β^--decay continuum spectrum of ^{138}La in sect. **3**. In the same section, the used experimental set-up and the description of the data set will be given. The results obtained from the data analysis will be described in sect. **4** while the conclusion of the work will be discussed in sect. **5**.

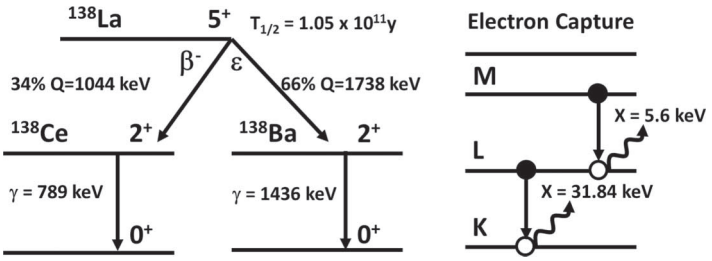

Fig. 1. – On the left: the decay scheme of the ^{138}La. It decays β^- to an excited state of ^{138}Ce with a probability of 34%, with the subsequent emission of a γ ray of 789 keV and alternatively ^{138}La decays, by electron capture, to an excited state of ^{138}Ba with a probability of 66%, with the subsequent emission of a γ ray of 1436 keV. On the rigth: The electron capture shell refilling. The electrons have to be re-adjusted after the decay, therefore there is an emission of an Auger electron of 5.6 keV, if the capture happens in the L shell, while there is a X-ray of 31.84 keV and the Auger electron emission, if the capture happens in the K shell.

2. – ^{138}La radioactive decay

Lanthanum is present in nature with two different isotopes: ^{139}La, that is stable and, ^{138}La, that has a lifetime of $1.05 \cdot 10^{11}$ years. The isotopic abundance of ^{138}La is 0.09% of the natural lanthanum. The ^{138}La isotope is an odd-odd p-nuclide produced by re-processing pre-existing seed nuclei created in the s- and r-processes. As a natural result the p-process nuclides are neutron-deficient and extremely rare in natural abundance.

The ^{138}La decays by electron capture ϵ into an excited state of ^{138}Ba with 66.4% probability and the remaining 33.6% by β^--decay into an excited state of ^{138}Ce [2]. In both cases, ^{138}La decays into an excited state of the daughter nucleus with the consequent emission of one gamma ray, as shown in fig. 1. In particular, one gamma ray of 1436 keV is emitted in the electron capture decay, while one gamma ray of 789 keV is emitted in the β^--decay process. Both the ^{138}La β^-- radioactive decay and electron capture are a 2nd-order unique forbidden transition (in both cases the decay starts from a 5^+ state ending to a 2^+ state). The Q-value of the β^--decay is 1044 keV. In the β^--decay a β particle, an antineutrino and a γ ray are emitted. The sum of β particle and the antineutrino energy is 255 keV ($E_{max\beta} = 1044$ keV–789 keV = 255 keV).

After the electron capture, the electrons have to be re-adjusted, therefore there is an X-ray and Auger electron emission (shell refilling). In particular, there is an Auger electron emission of 5.6 keV, if the captured electron was in the L shells, while there is a X-ray emission of 31.84 keV, if the captured electron was in the K shells, in this case there is also the emission of the Auger electron of 5.6 keV.

3. – Experimental set-up and method

Since only few years large volume $LaBr_3$:Ce are available as scintillator detectors. These scintillators are characterized by an intrinsic activity due to the presence of ^{138}La. This decay dominates the spectral region below 1.5 MeV. These large volume scintillators contain an amount of ^{138}La that is equal to its isotopic abundance. The used crystals were $3'' \times 3''$ and they contain about 10^{21} atoms of ^{138}La, that is approximately 1.5 g. For this reason, $LaBr_3$:Ce detectors offers an unique opportunity to measure the β^- continuum spectrum of ^{138}La. Furthermore, the $LaBr_3$:Ce scintillator presents excellent

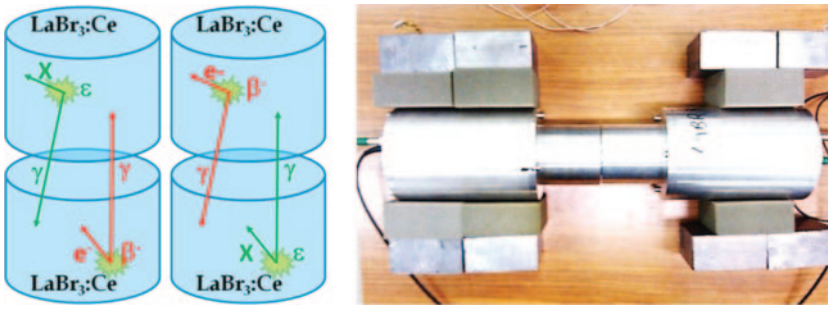

Fig. 2. – Rigth panel: the coincidence measurement technique. If a β^--decay occurs, the electron is detected in the $LaBr_3$:Ce where the decay has taken place, while the gamma ray of 789 keV could be detected in the other detector. If an electron capture occurs, in the $LaBr_3$:Ce where the decay has taken place the X-rays and Auger electrons are detected, while the gamma ray of 1436 keV could be detected in the other crystal. Left panel: a picture of the configuration of the two detectors, used during the two measurements.

scintillation properties. It has an extremely high light yield (63 photons/keV), the best energy resolution among scintillators (2.7% a 662 keV for small volume crystals), excellent timing properties (300 ps of time resolution in small crystals) and a high density (5.1 g/cm^3) [3-5]. For this reason the $LaBr_3$:Ce scintillator can be used, both as the ^{138}La source and as the detector to measure the β^- continuum spectrum.

The measurement of the β^--decay Continuum Spectrum of ^{138}La, requires a coincidence measurement. In the ^{138}La β^--decay one β particle, one γ-ray, and one anti-neutrino are emitted. The detection of the 789 keV γ-ray in one of the $LaBr_3$:Ce scintillator has to be in coincidence with an event in the second scintillator, that is the electron emitted in the β^--decay as shown in fig. 2. It is therefore possible to measure the electron continuum spectrum using the condition that a gamma-ray of 789 keV is measured in coincidence. The ^{138}La electron capture decay constitutes a source of background in this type of measurement.

The β^-- continuum spectrum of the ^{138}La was measured using two $3'' \times 3''$ $LaBr_3$:Ce detectors in coincidence, as shown in fig. 2. The detectors were coupled to an HAMAMASTU R6233-100sel PMT and to a standard HAMAMATSU voltage divider (E1198-26 and E1198-27). In the measurement the coincidence was produced using a constant fraction discriminator (Ortec Quad CFD 935) and a time to amplitude converter (TENNELEC TC 863). In this case it was possible to measure the spectrum starting from 30 keV, because of the CFD threshold. The two anode and the TAC signals were digitized using a 12 bit, 600 MHz LeCroy Waverunner HRO 66Zi. The acquisition trigger (trigger of the oscilloscope) was the TAC signal. The measurement provided two spectra, one for each detector. The acquisition time was about 4 days.

4. – Results

In the coincidence matrix of fig. 4 on the x-axis it is reported the energy measured in one of the detectors, while on the y axis the energy measured in the other one. To reduce the random coincidence the matrix was produced with a time condition of 3 ns around the prompt gamma peak, shown in fig. 3. The measured time resolution is about 2.3 ns. The time spectrum is obtained from the detector anode pulses with a digital

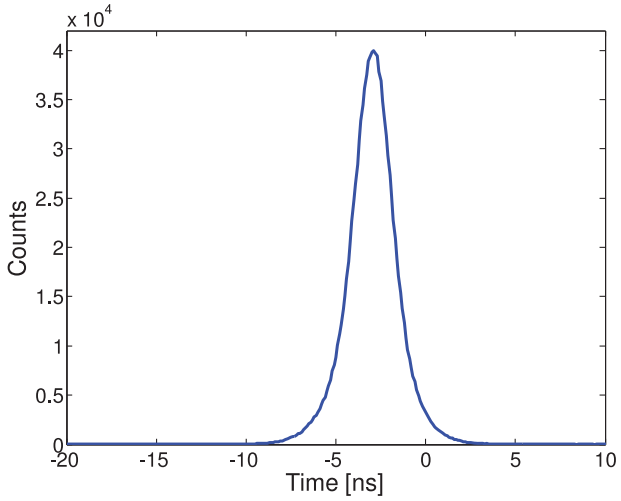

Fig. 3. – The measured time spectrum. The time spectrum was obtained from the anode signals of the detectors by a digital timing algorithm.

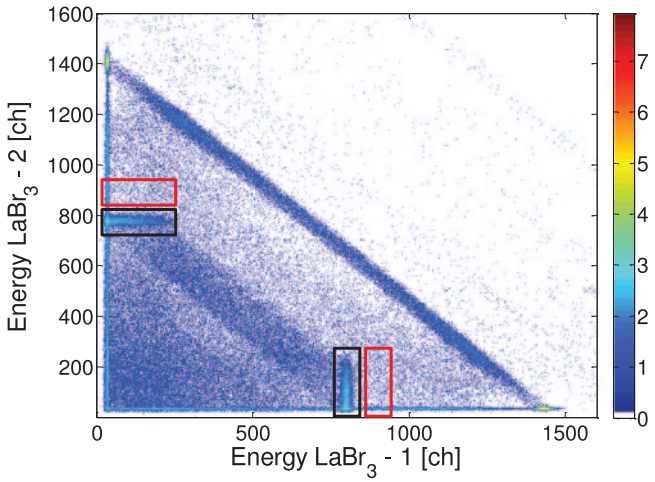

Fig. 4. – The coincidence matrix. The black squares indicate the gate on the 789 keV gamma ray, while the red ones are the gate used to subtract the background, owing to the Compton scattering of 1436 keV. It is reported the logarithm of the coincidence matrix.

timing algorithm. It is important to point out that the events outside the time peak are $< 0.1\%$.

The energy spectra of the two detectors were calibrated using standard gamma-ray sources (^{60}Co and ^{22}Na). The 789 keV peak was used to check the calibration and the drifts during all the measurement time. An important issue that must be taken in account is the scintillation non-proportional response, at low energies. It provides a visible distortion from a linear energy calibration of the spectrum. This non-proportional response was corrected by using the curve reported in [6].

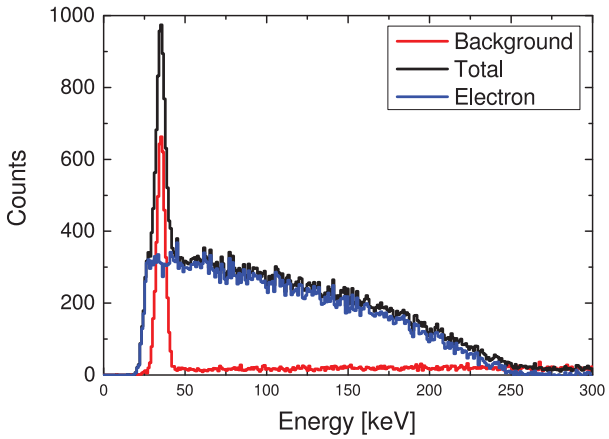

Fig. 5. – The spectrum associated to the coincidence with the gamma transition at 789 keV is indicated by the black line. The background spectrum is obtained by the coincidence with the Compton scattering of 1436 keV and it is shown with red line. The electron spectrum produces as the difference between the total spectrum and the background one is indicated by the blue line.

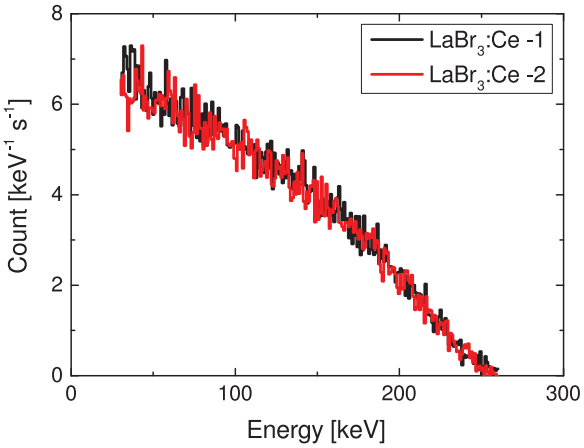

Fig. 6. – The β^--decay spectra of the two detectors are compared.

The total spectrum, reported in fig. 5 (black line), is the spectrum measured in one $LaBr_3$:Ce in coincidence with the transition at 789 keV, in the other one. The gates used to produce this spectrum are shown in fig. 4, indicated by a black squares. The 37.44 keV peak (that is the sum of the 31.84 keV X-ray plus the 5.6 KeV Auger electron) is evident in the spectrum associted to the black gate of fig. 4. This peak is from the K and L shell refelling of the electron capture and not from the β^--decay. It is present because of the Compton edge of the 1436 keV, that is also present in the region under the 789 keV, that has to be subtracted. The background spectrum, indicated in red in fig. 5, is obtained using the event in the red square of fig. 4. In that region, it is present only the Compton scattering of 1436 keV gamma ray. The measured electron spectrum, the blue line in fig. 5 is the difference between the total spectrum (black line) and the background one (red line).

As a cross-check, β^- spectrum of one detector is compared with the one obtained with the other one. The β^--decay spectrum has the same structure in both detectors, as shown in fig. 6. This implies that the spectra of the two detectors can be summed to increase the statistics. The final e^- spectrum was obtained by summing the spectra of the two $LaBr_3$:Ce detectors.

5. – Conclusion and perspectives

The measured β^- continuum spectrum, shown in fig. 6, is comparable to the experimental data present in literature. It has a different behavior at low energy (below 75 keV) with respect to the spectrum predicted by the theory, reported in [1].

A new measurement will be performed using digital electronics and exploiting the coincidence between an HPGe and a $LaBr_3$:Ce detector. The advantage of using a HPGe detector is the energy resolution of HPGe detector that is 10 time better than $LaBr_3$:Ce one. This energy resolution will provide a more precise coincidence with the 789 keV peak.

* * *

The project is co-financed by the European Union and the European Social Fund. This work was also supported by NuPNET - ERA-NET within the NuPNET GANAS project, under grant agreement No. 202914 and from the European Union, within the "7th Framework Program" FP7/2007-2013, under grant agreement No. 262010 - ENSAR-INDESYS.

REFERENCES

[1] Quarati F. *et al.*, *Nucl. Instrum. Methods A*, **683** (2012) 46.
[2] Firestone J. R. B., *Table of Isotopes*, 8th edition (Wiley-VCH), 1999 available from:/ `http://ie.lbl.gov/toi.htlm`.
[3] Nicolini R. *et al.*, *Nucl. Instrum. Methods A*, **582** (2007) 554.
[4] Quarati F. *et al.*, *Nucl. Instrum. Methods A*, **574** (2007) 115.
[5] Giaz A. *et al.*, *Nucl. Instrum. Methods A*, **729** (2013) 910.
[6] Alekhin M. S. *et al.*, *Appl. Phys. Lett.*, **102** (2013) 161915-1.